THE GEOLOGICAL SOCIETY OF AMERICA®

Seismic array constraints on reach-scale bedload transport

B. Schmandt[1], D. Gaeuman[2], R. Stewart[2], S.M. Hansen[1], V.C. Tsai[3], and J. Smith[1]
[1]Earth and Planetary Science Department, University of New Mexico, Albuquerque, New Mexico 87131, USA
[2]Trinity River Restoration Program, Weaverville, California 96093, USA
[3]Seismological Laboratory, California Institute of Technology, Pasadena, California 91125, USA

ABSTRACT

Measurements and mechanical models of heterogeneous bedload transport in rivers remain basic challenges for studies of landscape evolution and watershed management. A 700 m reach of the Trinity River (northern California, USA), a large gravel-bed river, was instrumented with an array of 76 seismographs during a dam-controlled flood and gravel augmentation to investigate the potential for out-of-stream monitoring. The temporal response to gravel augmentation during constant discharge provides strong evidence of seismic sensitivity to bedload transport and aids in identification of the seismic frequencies most sensitive to bedload in the study area. Following gravel augmentations, the seismic array reveals a period of enhanced transport that spans most or all of the reach for ~7–10 h. Neither the duration nor the downstream extent of enhanced transport would have been constrained without the seismic array. Sensitivity to along-stream transport variations is further demonstrated by seismic amplitudes that decrease between the upper and lower halves of the reach consistent with decreased bedload flux constrained by time-lapse bathymetry. Insight into the magnitude of impact energy that reaches the bed is also gained from the seismic array. Observed peak seismic power is ~1%–5% of that predicted by a model of saltation over exposed bedrock. Our results suggest that dissipation of impact energy due to cover effects needs to be considered to seismically constrain bedload transport rates, and that noninvasive constraints from seismology can be used to test and refine mechanical models of bedload transport.

INTRODUCTION

Mechanical work done at Earth's surface by erosional processes can contribute to the signals recorded by ground velocity sensors in seismographs. Application of seismology to monitoring surface processes has expanded recently, including studies of rivers, landslides, debris flows, glaciers, and coastal processes (e.g., Burtin et al., 2016; Larose et al., 2015; Kean et al., 2015; Gimbert et al., 2016; Poppeliers and Mallinson, 2015). Bedload transport in rivers is a particularly relevant target for seismology because it is an important component of sediment transport and river incision that is difficult to measure (e.g., Gray et al., 2010), especially during high discharge events, and the abundant collisions between coarse grains and the riverbed are predicted to yield measurable seismic waves outside the channel (Tsai et al., 2012).

Seismic detection of coarse sediment transport has been suggested based on hysteresis in observed seismic power versus water discharge, which likely represents variable bedload transport for a given discharge owing to temporally evolving bedload supply (Burtin et al., 2008; Hsu et al., 2011; Schmandt et al., 2013; Díaz et al., 2014; Roth et al., 2014; Chao et al., 2015). However, the utility of detecting bedload by observing hysteresis is limited because all bedload transport events need not exhibit hysteresis and changes in bed morphology could contribute to hysteresis by changing turbulent flow (Gimbert et al., 2014). Comparisons of continuous seismic amplitudes with physical bedload samples (Burtin et al., 2011), proxies from acoustic monitoring of impact plates beneath the riverbed (e.g., Barrière et al., 2015; Roth et al., 2016), and flux measured by direct capture (Roth et al., 2016) also provide evidence that bedload is seismically detectable. Remaining challenges that we seek to address include the robust separation of water and bedload signals (Roth et al., 2016), a paucity of constraints on how seismic signals vary along stream, and the need to test mechanical models of the seismic signal of bedload.

Here we take advantage of extensive monitoring and regulation of the Trinity River in northern California, as part of the Trinity River Restoration Program (Gaeuman, 2014), to investigate fluvial seismic signals during a dam-controlled flood and controlled gravel augmentation. In particular, we seek to study the temporal and spatial scales of enhanced bedload transport due to gravel augmentation. Knowledge of those scales is valuable for management decisions, but they are poorly constrained by conventional methods. Advancing upon prior seismic studies we use an array of 76 seismographs to continuously monitor along-stream variations in seismic signals (Fig. 1). Complementary constraints include a local gage station, time-lapse bathymetry, and physical sampling of bedload. Our results deliver new constraints on the duration and downstream extent of enhanced bedload transport, demonstrate seismic sensitivity to reach-scale transport variations, and reveal low seismic power compared to predictions for a model of saltation in a bedrock channel.

DATA

Seismic data were collected during a dam-controlled flood in May 2015. Small cable-free seismographs referred to as nodes were used to

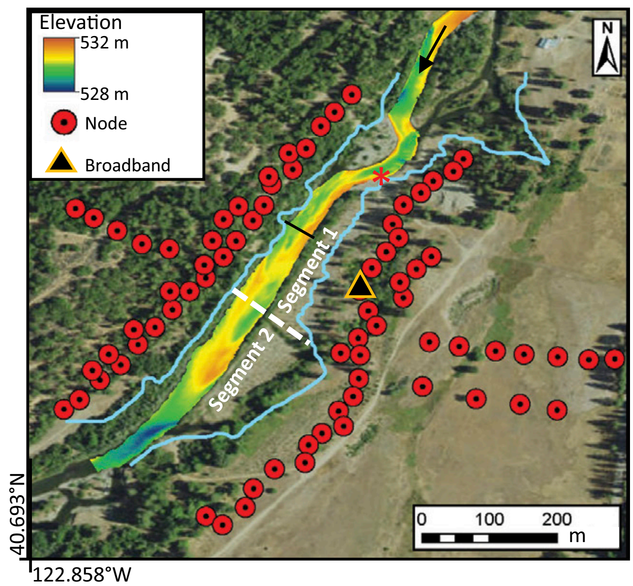

Figure 1. Map of the study reach. Node and broadband seismograph locations are indicated. The physical sampler transect is labeled in black. The high water line at peak discharge is contoured in blue. The red asterisk denotes the gravel injection point. Sonar-constrained bathymetry is shown for the deepest part of the channel. River flow direction is indicated by the black arrow.

Data Repository item 2017088 | doi:10.1130/G38639.1

form a 76 element array spanning a 700 m reach of the Trinity River (Fig. 1). Each node contained a 10 Hz geophone sensitive to vertical ground motion, and an additional broadband seismometer was installed near the middle of the array (see the GSA Data Repository[1]). Analysis was restricted to nighttime measurements, 7:00 p.m. to 7:00 a.m. local time (Greenwich Mean Time, GMT–7 h), because of interference from anthropogenic signals within the study area and on nearby roads during the day. Water discharge was controlled by the release at Lewiston Dam, no rainfall occurred during the flood, and estimated discharge uncertainty at the gage station in the study area is <10% (see Data Repository Fig. DR1).

Gravel augmentation was conducted by deposition from a front-end loading tractor near the outside of a river bend at the upstream end of the reach (Fig. 1). Each of the two injection events deposited 260 m^3 in 60 loads over 2 h. The first injection occurred near the end of the rising limb of the hydrograph and the second occurred during constant peak discharge of ~235 m^3/s (Fig. 2B). Consistent with prior controlled floods at the Trinity River (Gaeuman, 2014), bedload was monitored with time-lapse bathymetry and physical sampling across a transect ~150 m downstream from the injection point (Fig. 1).

Physical sampling was conducted with a Toutle River 2 sampler using an average of 11 equally spaced placements across the transect to estimate the bedload transport rate and grain-size distribution 5–6 times each day (Fig. 1; see the Data Repository). During the 3 days of highest discharge, when nearly all transport occurred, the mean estimated transport rate averaged across the transect was 3.9 kg/s and the maximum was 12 kg/s (Fig. DR3). The sampled bedload was primarily gravel; 85% of the sampled mass consisted of >2 mm grains. The D_{50}, D_{90}, and D_{95} of sampled grains were 27, 76, and 87 mm, respectively. We use the physical sampler data for grain-size constraints and approximate bounds on bedload transport rates, but we do not analyze the temporally coincident seismic data because the sampling activity and other daytime signals interfere with seismic measurements.

[1]GSA Data Repository item 2017088, additional presentation of data and methods, is available online at http://www.geosociety.org/datarepository/2017/, or on request from editing@geosociety.org.

Constraints on bedload flux are also obtained from time-lapse bathymetry, which was surveyed four times (B1–B4) during the flood by boat-mounted sonar sounding (Gaeuman, 2014; Fig. DR2). An additional survey from 2011 (B0) was used to constrain cumulative changes during this event because the first survey in 2015 was conducted when discharge already exceeded the threshold for gravel transport of ~110 m^3/s (see the Data Repository). Differential bathymetry is primarily sensitive to gravel flux because the riverbed is composed of clast-supported gravel and cobbles (Viparelli et al., 2011), and the small fraction of sand occupies pore spaces between larger grains (Gaeuman, 2014). Differential bathymetry indicates that the reach accumulated ~1210 m^3 of gravel, which places a lower bound on bedload transport into the reach, neglecting gravel that passed through the entire reach. The estimate of cumulative bedload transport from physical sampler data is 23% lower than the estimate from differential bathymetry, and about half that difference can be accounted for by a small bedload transport event in 2012 (see the Data Repository). The approximate agreement between the two estimates suggests it is unlikely that a large fraction of transported gravel passed through the entire reach.

IDENTIFICATION OF WATER AND BEDLOAD SIGNALS

The broadband seismograph's vertical amplitude spectra during three time periods (S1, S2, S3) illustrate the frequencies dominantly excited by water and bedload transport (Fig. 2A). The S1 spectrum (Fig. 2A) was observed at 11:00 p.m. prior to the controlled flood during discharge of 107 m^3/s. It serves as a reference spectrum because no gravel transport occurs in the reach below ~110 m^3/s (Gaeuman, 2014; Fig. DR3). The S2 spectrum was observed on day 126 during peak discharge of 235 m^3/s and 2 h after the second gravel injection (Fig. 2C). It approximates the maximum 3–100 Hz signal at this seismograph during the experiment. The S3 spectrum was observed 6 h after the S2 spectrum at equal discharge. Gravel injection during constant discharge provides an opportunity to isolate the frequency range that responds to bedload supply variations. The power decrease during the night of constant discharge, represented by the difference between S2 and S3, is at least 50% greater than S3 for frequencies >20 Hz (Fig. DR4). Consequently, we focus on frequencies >20 Hz as a potential bedload transport proxy.

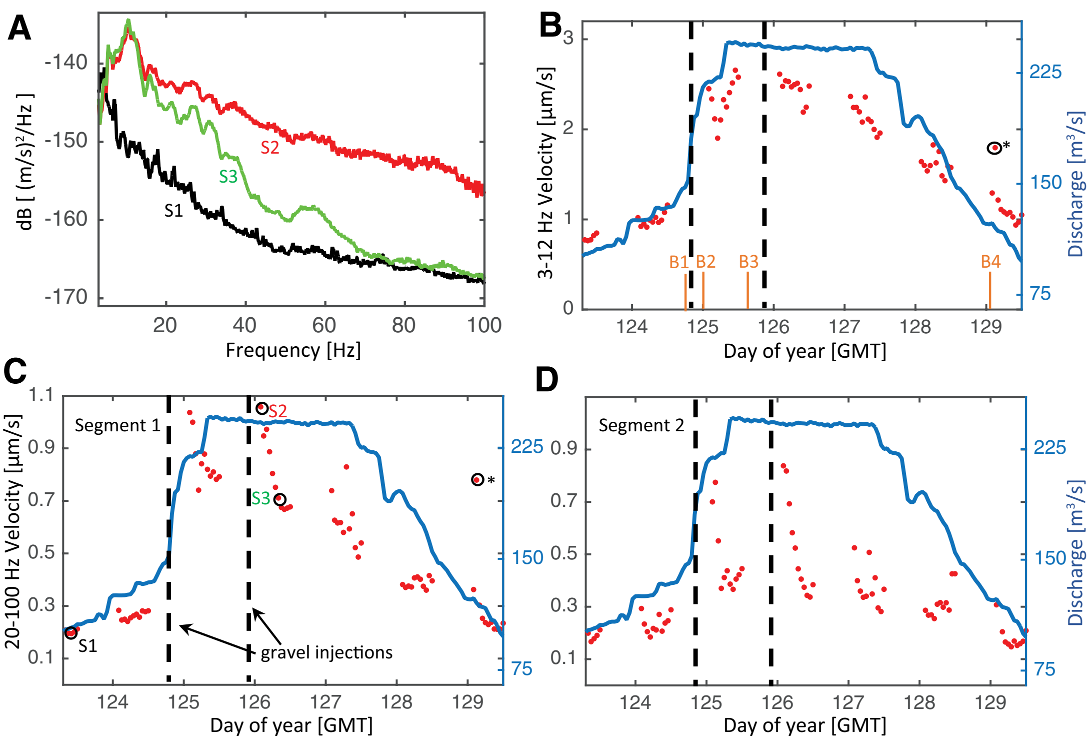

Figure 2. Seismic response to controlled flood and gravel injections. A: Vertical power spectral density at the broadband seismograph during three time periods, S1, S2, and S3 are labeled in A and C. B: Lower frequency band, 3–12 Hz; hourly amplitudes averaged across the entire reach are shown with red dots, and the blue line shows the water discharge. In B–D, the vertical black dashed lines denote gravel injections. The orange vertical line segments denote the four bathymetric surveys (B1–B4) during the flood. The black asterisk denotes anomalous amplitude when a motorized boat was in operation. GMT—Greenwich Mean Time. C: Higher frequency band, 20–100 Hz; hourly amplitudes in reach segment 1. The locations of segments 1 and 2 are labeled in Figure 3. D: Higher frequency band hourly amplitude in segment 2.

Distinct temporal variations in seismic amplitude in two frequency bands illustrates their dominant sensitivity to fluid and bedload transport, respectively. Hourly seismograms were bandpass filtered between 3–12 Hz and 20–100 Hz, and the hourly median amplitude was computed for each node. Mean amplitude across the array in the 3–12 Hz band varied smoothly with water discharge exhibiting a linear correlation coefficient of 0.96 and a lack of strong responses to gravel injections (Fig. 2B). In contrast, 20–100 Hz amplitudes peaked after each gravel injection and then decayed for ~7–10 h (Figs. 2C and 2D). The first postinjection amplitude decay occurred during rising discharge and the second occurred during constant discharge, providing strong evidence that they are linked to bedload rather than water transport.

TEMPORAL AND SPATIAL SCALES OF RESPONSE TO GRAVEL INJECTIONS

The array was separated into two segments to investigate the extent of the reach affected by gravel augmentation (Fig. 2). Seismic waves from the river propagate in all directions, so signals in the two segments are not entirely independent. However, observed amplitude decay with distance orthogonal to the channel indicates that >20 Hz amplitudes are dominated by sources within each segment (Fig. DR6). Both segments exhibited amplitude maxima following gravel injections, but the amplitude range following gravel augmentation was smaller in segment 1, which contains the injection site (Fig. 2C). Postinjection amplitude decay occurred over the first ~4–7 h of the night, which corresponds to ~7–10 h after injection. We also tested separating the channel into 3 equal length segments and found similar results, indicating that the transient response spanned most or all of the 700 m reach (Fig. DR7).

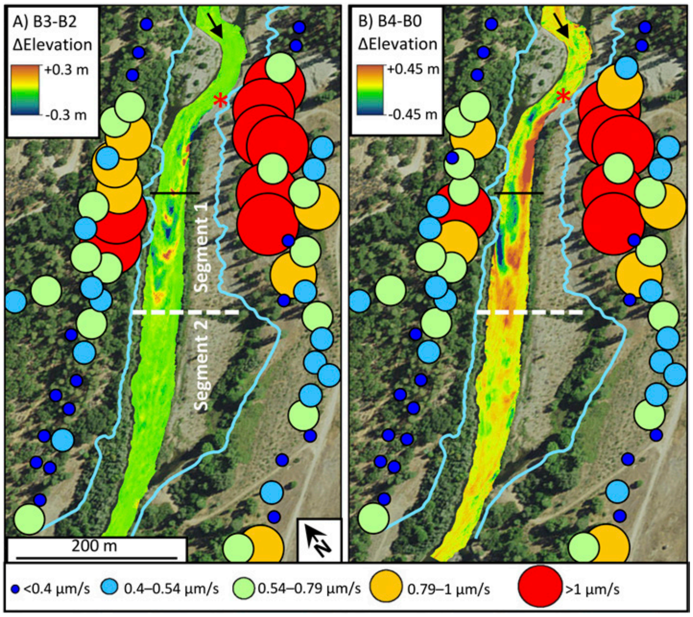

Figure 3. Spatial distributions of seismic amplitudes and bathymetric changes. A: Differential bathymetry from sonar survey B3–B2 corresponds to nighttime changes following the first gravel injection. Node seismographs symbol size and color correspond to nighttime median 20–100 Hz following the first day of the flood. The red asterisk denotes the gravel injection point. B: Differential bathymetry shows the change in bed elevation between survey B4 in 2015 and survey B0, which was conducted in 2011. Median seismic amplitudes through the three nights of highest discharge are plotted.

ALONG-STREAM SEISMIC AMPLITUDES AND BEDLOAD TRANSPORT

Maps of time-averaged amplitude at each node identify along-stream variability similar to an along-stream change in gravel accumulation revealed by time-lapse bathymetry (Fig. 3). Higher seismic amplitudes were observed in the upstream segment of the reach (segment 1) compared to the downstream half of the reach (segment 2). The highest amplitudes were observed between the gravel injection site and ~250 m downstream, where migrating ~0.2–0.4-m-tall bedforms were detected by differential bathymetry (Fig. 3A). This amplitude pattern was similar for the first night of peak discharge and the three night mean. Node distances from the thalweg were greater in segment 2, but after correction for distance segment 1 mean amplitude was still 66% greater than in segment 2 (Fig. DR6). A similar difference between segments 1 and 2 was observed in gravel accumulation (Figs. 3A and 3B). Differential bathymetry shows that most gravel accumulation, ~980 m^3 of the total ~1210 m^3, occurred in segment 1. Thus, the lower bound on bedload flux from time-lapse bathymetry suggests a factor of ~5 downstream decrease in gravel transport from segment 1 to 2, consistent with bedload flux as a cause of along-stream seismic amplitude variations. Net accumulation of gravel is likely because the study reach slope of 0.0012 is lower than the average slope of 0.0023 between the dam and the study area.

DISCUSSION

Seismic frequencies lower than ~12 Hz are interpreted as dominantly sensitive to water transport because of their correlation with discharge and relative lack of response to gravel injections (Fig. 2B; Fig. DR4). Transient responses to increased gravel supply provide clear evidence that out-of-stream seismic monitoring is sensitive to variations in bedload transport, particularly for frequencies of ~20–100 Hz at our study location (Figs. 2C and 2D). While gravel augmentation can locally affect bed roughness and consequently water turbulence (Gimbert et al., 2014), observation of a high-frequency seismic response along the entire reach, including areas with nearly constant bathymetry, indicates that bedload rather than turbulence is the dominant cause of the seismic transients. Our observation of bedload supply augmentation during constant discharge is novel, and it strengthens evidence that ~15–100 Hz seismic signals observed within ~10–100 m of streams are sensitive to bedload (e.g., Roth et al., 2016; Burtin et al., 2016; Schmandt et al., 2013; Barrière et al., 2015).

The new seismic array data provide otherwise unavailable constraints on the temporal and spatial scales affected by regulated high discharge and gravel injection in the Trinity River, and are important for assessing contributions to management goals for physical habitat (e.g., Gaeuman, 2014). Observations of similar peak amplitude and duration seismic transients in both upstream and downstream halves of the reach suggest that the local increase in gravel supply stimulated a short-term, ~7–10 h, increase in bedload transport along most or all of the ~700 m reach. Transient seismic amplitude increases in the downstream half of the reach decayed to lower values than in the upstream half, suggesting a longer term effect within ~250 m of the injection site where migrating bedforms were observed (Fig. 3A). Analogous migrating bedforms superimposed on alternating bar bathymetry have been found in flume experiments simulating bedload supply augmentation (Podolak and Wilcock, 2013).

The results of this experiment offer opportunities to test a recent physical model of the seismic signal of bedload (Tsai et al., 2012) with observations of both along-stream variations and absolute power levels. Differential bathymetry indicates that bedload transport decreased downstream by a factor of ~5 from segment 1 to 2 (Fig. 3B), and the Tsai et al. (2012) model of saltation over exposed bedrock predicts that seismic power is proportional to mass transport rate. The observed ratio of mean power in segment 1–2 from 20 to 100 Hz was 2.4, which is somewhat lower than the expected factor of 5 based on differential bathymetry. Minor mixing of signals between segments, the model's simplifying assumptions, and inaccuracy of input parameters are potential sources of the modest discrepancy. Specifically, the model assumes saltation-dominated transport, but different mechanisms such as rolling and sliding can alter bedload impact energy (Turowski et al., 2015) and their relative importance could vary along stream. The presence of migrating bedforms in only the upstream segment of the reach is a simple indication that the assumption of uniform transport mechanics may be inadequate. Model application to along-stream variations is also challenged by the lack of constraint on along-stream variations of input parameters, particularly grain size. Predicted power is proportional to grain size cubed, so the model is very sensitive to the input of effective grain size ~D_{94} (Chao et al., 2015). The standard deviation of D_{95} at the physical sampler transect is 18.5 mm, which is sufficient uncertainty to change the predicted power by a factor of ~2. Thus, the seismic array and bathymetry results suggest that reach-scale bedload variations are detectable, but models suited to local transport mechanisms and spatially varying input parameters may be needed for accurate predictions or inversions.

Riverside measurements of absolute seismic power provide feedback for mechanical models of bedload transport by constraining impact energy transmitted to the bed. We find that observed peak seismic power is ~1%–5% of that predicted for the saltation-dominated bedrock channel case using the model of Tsai et al. (2012) (Fig. DR8). This discrepancy implies greater dissipation of initial impact energy and/or lower impact energy per unit mass transport. First, the gravel bed of the study reach is a poor fit to the assumption of an exposed bedrock channel, and coarse unconsolidated sediments can strongly dissipate seismic energy (e.g., Mavko et al., 2009), consistent with experimental studies of cover effects (e.g., Turowski and Bloem, 2016). Second, streambed impact-plate studies indicate that bedload impact energy varies among transport mechanisms including saltation, rolling, and sliding (Turowski et al., 2015). However, our assumption of transport by saltation is expected to underestimate impact energy (Turowski et al., 2015), rather than overestimate it. We suggest that neglect of seismic energy dissipation due to cover effects is the clearest shortcoming of the model for our study area, and that incorporation of cover effects, which may vary along stream, should be considered in future mechanical models.

CONCLUSIONS

Seismic array observations of a regulated flood and gravel supply augmentation have shown that seismic monitoring is sensitive to temporal and spatial variations in bedload transport down to the reach scale. The seismic data constrained the time scale and spatial extent of enhanced transport in response to augmentation, neither of which would have been delimited without the seismic array, and both are valuable for future management efforts. The new array data also revealed challenges in mechanical modeling of bedload transport and inverting seismic signals for mass transport rates in diverse rivers. Observed peak seismic power was ~1%–5% of that predicted by a theoretical model of saltation in a bedrock channel, indicating that cover effects in gravel-bed streams and potential contributions from mechanisms other than saltation should be considered to obtain accurate estimates of bedload flux from seismic data.

ACKNOWLEDGMENTS

Seismic data will be openly available through the Incorporated Research Institutions for Seismology Data Management Center (http://ds.iris.edu/ds/nodes/dmc/) beginning in May 2017. Trinity River Restoration Program water and sediment transport data are openly available (http://www.trrp.net). J. Turowski and T. Batholomaus provided helpful reviews. Support from National Science Foundation grant 1554908 (to Schmandt) and grant 1453263 (to Tsai) is acknowledged.

REFERENCES CITED

Barrière, J., Oth, A., Hostache, R., and Krein, A., 2015, Bed load transport monitoring using seismic observations in a low-gradient rural gravel bed stream: Geophysical Research Letters, v. 42, p. 2294–2301, doi:10.1002/2015GL063630.

Burtin, A., Bollinger, L., Vergne, J., Cattin, R., and Nábělek, J.L., 2008, Spectral analysis of seismic noise induced by rivers: A new tool to monitor spatiotemporal changes in stream hydrodynamics: Journal of Geophysical Research, v. 113, B05301, doi:10.1029/2007JB005034.

Burtin, A., Cattin, R., Bollinger, L., Vergne, J., Steer, P., Robert, A., and Tiberi, C., 2011, Towards the hydrologic and bed load monitoring from high-frequency seismic noise in a braided river: The "torrent de St Pierre," French Alps: Journal of Hydrology, v. 408, p. 43–53, doi:10.1016/j.jhydrol.2011.07.014.

Burtin, A., Hovius, N., and Turowski, J.M., 2016, Seismic monitoring of torrential and fluvial processes: Earth Surface Dynamics, v. 4, p. 285–307, doi:10.5194/esurf-4-285-2016.

Chao, W.A., Wu, Y.M., Zhao, L., Tsai, V.C., and Chen, C.H., 2015, Seismologically determined bedload flux during the typhoon season: Scientific Reports, v. 5, 8261, doi:10.1038/srep08261.

Díaz, J., Ruíz, M., Crescentini, L., Amoruso, A., and Gallart, J., 2014, Seismic monitoring of an Alpine mountain river: Journal of Geophysical Research, v. 119, p. 3276–3289, doi:10.1002/2014JB010955.

Gaeuman, D., 2014, High-flow gravel injection for constructing designed in-channel features: River Research and Applications, v. 30, p. 685–706, doi:10.1002/rra.2662.

Gimbert, F., Tsai, V.C., and Lamb, M.P., 2014, A physical model for seismic noise generation by turbulent flow in rivers: Journal of Geophysical Research, v. 119, p. 2209–2238, doi:10.1002/2014JF003201.

Gimbert, F., Tsai, V.C., Amundson, J.M., Bartholomaus, T.C., and Walter, J.I., 2016, Subseasonal changes observed in subglacial channel pressure, size, and sediment transport: Geophysical Research Letters, v. 43, p. 3786–3794, doi:10.1002/2016GL068337.

Gray, J.R., Laronne, J.B., and Marr, J.D., 2010, Bedload-surrogate monitoring technologies: U.S. Geological Survey Scientific Investigations Report 2010–5091, 37 p.

Hsu, L., Finnegan, N.J., and Brodsky, E.E., 2011, A seismic signature of river bedload transport during storm events: Geophysical Research Letters, v. 38, L13407, doi:10.1029/2011GL047759.

Kean, J.W., Coe, J.A., Coviello, V., Smith, J.B., McCoy, S.W., and Arattano, M., 2015, Estimating rates of debris flow entrainment from ground vibrations: Geophysical Research Letters, v. 42, p. 6365–6372, doi:10.1002/2015GL064811.

Larose, E., Carrière, S., Voisin, C., Bottelin, P., Baillet, L., Guéguen, P., and Gimbert, F., 2015, Environmental seismology: What can we learn on earth surface processes with ambient noise?: Journal of Applied Geophysics, p. 116, v. 62–74, doi:10.1016/j.jappgeo.2015.02.001.

Mavko, G., Mukerji, T., and Dvorkin, J., 2009, The rock physics handbook: Tools for seismic analysis of porous media: New York, Cambridge University Press, 524 p, doi:10.1017/CBO9780511626753.

Podolak, C.J.P., and Wilcock, P.R., 2013, Experimental study of the response of a gravel streambed to increased sediment supply: Earth Surface Processes and Landforms, v. 38, p. 1748–1764, doi:10.1002/esp.3468.

Poppeliers, C., and Mallinson, D., 2015, High-frequency seismic noise generated from breaking shallow water ocean waves and the link to time-variable sea states: Geophysical Research Letters, v. 42, p. 8563–8569, doi:10.1002/2015GL066126.

Roth, D.L., Finnegan, N.J., Brodsky, E.E., Cook, K.L., Stark, C.P., and Wang, H.W., 2014, Migration of a coarse fluvial sediment pulse detected by hysteresis in bedload generated seismic waves: Earth and Planetary Science Letters, v. 404, p. 144–153, doi:10.1016/j.epsl.2014.07.019.

Roth, D.L., Brodsky, E.E., Finnegan, N.J., Rickenmann, D., Turowski, J.M., and Badoux, A., 2016, Bed load sediment transport inferred from seismic signals near a river: Journal of Geophysical Research, v. 121, p. 725–747, doi:10.1002/2015JF003782.

Schmandt, B., Aster, R.C., Scherler, D., Tsai, V.C., and Karlstrom, K., 2013, Multiple fluvial processes detected by riverside seismic and infrasound monitoring of a controlled flood in the Grand Canyon: Geophysical Research Letters, v. 40, p. 4858–4863, doi:10.1002/grl.50953.

Tsai, V.C., Minchew, B., Lamb, M.P., and Ampuero, J.P., 2012, A physical model for seismic noise generation from sediment transport in rivers: Geophysical Research Letters, v. 39, L02404, doi:10.1029/2011GL050255.

Turowski, J.M., and Bloem, J.-P., 2016, The influence of sediment thickness on energy delivery to the bed by bedload impacts: Geodinamica Acta, v. 28, p. 199–208, doi:10.1080/09853111.2015.1047195.

Turowski, J.M., Wyss, C.R., and Beer, A.R., 2015, Grain size effects on energy delivery to the streambed and links to bedrock erosion: Geophysical Research Letters, v. 42, p. 1775–1780, doi:10.1002/2015GL063159.

Viparelli, E., Gaeuman, D., Wilcock, P.R., and Parker, G., 2011, A model to predict the evolution of a gravel bed river under an imposed cyclic hydrograph and its application to the Trinity River: Water Resources Research, v. 47, W02533, doi:10.1029/2010WR009164.

Manuscript received 26 September 2016
Revised manuscript received 27 November 2016
Manuscript accepted 4 December 2016

Printed in USA